

Traffic-Aware Vehicle Energy Management Strategies via Scenario-Based Optimization^{*}

L.A. Wulf Ribelles G.P. Padilla M.C.F. Donkers

*Dept. Electrical Eng, Eindhoven University of Technology, Netherlands
(e-mail: l.a.wulf.ribelles@student.tue.nl, {g.p.padilla.cazar, m.c.f.donkers}@tue.nl)*

Abstract: This paper explores the development of traffic-aware energy management strategies by means of scenario-based optimization. This is motivated by that fact that real driving conditions are subject to uncertainty, thereby making the real-time optimization of the energy consumption of a vehicle to be a challenging problem. In order to deal with this situation, we employ the current framework of complete vehicle energy management in a receding horizon fashion, in which we consider random constraints representing realizations of exogenous signals, i.e., the uncertain driving conditions. Additionally, we study three methods for velocity prediction in energy management strategies, i.e., a method based on (average) traffic flow information, a method based on Gaussian process regression, and a method that combines both. The proposed strategy is tested with real traffic data using a case study of the power split in a series-hybrid electric vehicle. The behavior of the battery, control inputs and fuel consumption generated with the resulting strategies are compared against the optimal solution from an offline benchmark and a situation with perfect prediction of the future. For the considered case, the use of a Gaussian process regression and the traffic speed achieves near optimal fuel consumption.

Keywords: Vehicle Energy Management, Model Predictive Control, Scenario Optimization, Power request predictions

1. INTRODUCTION

Nowadays, vehicle efficiency has become more relevant due to the need to mitigate the environmental impact of fossil fuels and to meet the CO_2 emission targets set for 2030 as expressed in the "Global EV Outlook 2018" and "IEA New Policies Scenario" (IEA, 2018). In fact, several countries are proposing regulations to stop the use of non-electrified vehicles in the city centers or even suggesting to ban the commercialization of petrol-based passenger cars between 2025 and 2040. However, e-mobility faces a crucial problem to experience a total incorporation in the transportation market denominated *range anxiety*, i.e., users are concerned about not having enough energy to reach their final destination (IEA, 2018). From this perspective, the development of Energy Management Strategies (EMSs) becomes a relevant research topic in the automotive industry, because their implementation does not require substantial hardware modifications to achieve longer traveling distances using only a reduced amount of energy.

Basically, EMSs determine how to optimize the energy consumption of a vehicle by establishing an appropriate division of the energy used by its components and subsystems, which in a broader sense is referred as Complete Vehicle Energy Management (CVEM) (Kessels et al.,

2012). Generally, the EMS literature can be divided into online and offline methods. Offline methods are typically based on Dynamic Programming, Pontryagin's Minimum Principle (Sciarretta and Guzzella, 2007) or static optimization techniques (Khalik et al., 2018; Padilla et al., 2019), and require the drive cycle to be known a priori. These methods are not real-time implementable and neglect the presence of uncertain driving conditions, e.g., traffic congestion, varying speed limits and different driving styles. Alternatively, different online methods explored in the literature are given by rule-based techniques, express the energy required by the subsystems through Equivalent Consumption Minimization Strategies (ECMS) (Sciarretta and Guzzella, 2007) or apply Model Predictive Control (MPC) methods with online predictions of the driving mission (Romijn et al., 2017).

Despite being online implementable, all these methods required tuning, which often relies on offline solutions, or assume exact predictions of the power request, limiting their use under real-life situations. Alternatively, stochastic optimal control methods provide noticeable extensions for Traffic-aware Energy Management Strategies (TaEMS), i.e., strategies that take into account the uncertainty present in real traffic conditions. These strategies are typically obtained using Stochastic Dynamic Programming (SDP) (Johannesson et al., 2007), which suffers from scalability problems known as "Curse of Dimensionality", or Stochastic MPC (Di Cairano et al., 2014), which could become computationally demanding when the number of subsystems considered in the control problem increases.

^{*} This work has received financial support from the Horizon 2020 program of the European Union under the grant 'Electric Vehicle Enhanced Range, Lifetime And Safety Through INGenious battery management' (EVERLASTING-713771).

In this paper, we use the recent developments of scenario-based optimization (Campi and Garatti, 2018; Schildbach et al., 2013, 2014) to extend the current framework of CVEM as in Padilla et al. (2019). This aims to achieve a tractable method for traffic-aware complete vehicle energy management, in which an intuitive tradeoff can be made between computational complexity and robustness depending on the number of scenarios considered. Furthermore, the proposed method has the potential of using distributed optimization techniques to improve its implementation capabilities (although this will not be addressed in this paper). In addition, we propose the use of Gaussian Processes Regression for this TaEMS to generate multiple predictions of the future driving situations, i.e., sample random scenarios, which are combined with traffic flow information to provide long-term speed predictions.

This paper is organized as follows: In Section 2, the general vehicle energy management problem formulation is presented and extended as an uncertain optimal control problem. A description of the prediction methods for traffic-aware vehicle energy management is included in Section 3. Section 4 presents the implementation details and simulation results obtained on a case study. Finally, conclusions are presented in Section 5.

2. TRAFFIC-AWARE VEHICLE ENERGY MANAGEMENT

In this section, we present the mathematical formulation describing the optimal control problem arising from the CVEM framework in a receding horizon fashion. Additionally, an extension of the resulting Receding-Horizon Optimal Control Problem (RHOC) in the context of scenario-based optimization is introduced to account for uncertain factors affecting a vehicle, i.e., the uncertain power request caused by, e.g., unknown driving conditions.

2.1 Receding Horizon Optimal Control Problem

In general, the CVEM problem aims to define the optimal energy flows between the subsystems in the power network of a vehicle over a prediction horizon $k \in \mathcal{K} = \{0, 1, \dots, K-1\}$ given the measurements at time step $t \in \mathbb{N}$ represented by

$$\min_{\{u_{m,k|t}, y_{m,k|t}, x_{m,k|t}\}} \sum_{m \in \mathcal{M}} \sum_{k \in \mathcal{K}} a_{m,k} y_{m,k|t} + b_{m,k} u_{m,k|t} \quad (1a)$$

where $x_{m,k|t} \in \mathbb{R}^{n_m}$ are the states, $u_{m,k|t} \in \mathbb{R}$ are scalar inputs and $y_{m,k|t} \in \mathbb{R}$ are scalar outputs of the converter of subsystem $m \in \mathcal{M} = \{1, \dots, M\}$, and the coefficients $a_{m,k} \in \mathbb{R}_{+0}$, $b_{m,k} \in \mathbb{R}$ define the desired cost metric based on the energy consumed by each subsystem at time instant $k+t$. For instance, setting all coefficients to zero apart from $a_{1,k}$ and assuming that $m=1$ corresponds to the combustion engine results in a fuel consumption minimization, where $y_{1,k|t}$ represents the chemical fuel power flow and $a_{1,k}$ can be either a constant or variable coefficient, e.g., sampling time. Note that the subscript $[\cdot]_{|t}$ will be dropped for clarity of the notation as the terms $\{u, y, x, w\}$ throughout this paper define predictions at time $k+t$ given information of time $t \in \mathbb{N}$ and $k \in \mathcal{K}$.

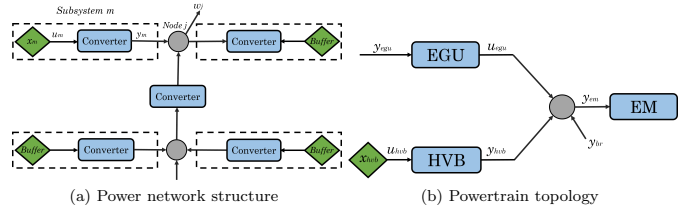


Fig. 1. CVEM diagrams.

The minimization of (1a) is subject to a set of constraints describing the behaviour of the vehicle's power network and the exchanges of power in it (Fig. 1a shows a general network structure). First, we consider quadratic equality constraints that define the input-output behaviour of the converter in each subsystem

$$y_{m,k} = \frac{1}{2} \gamma_{2,m} u_{m,k}^2 + \gamma_{1,m} u_{m,k} + \gamma_{0,m} \quad (1b)$$

with $\gamma_{2,m} \in \mathbb{R}_+$, $\gamma_{1,m} \in \mathbb{R}$ and $\gamma_{0,m} \in \mathbb{R}$ being coefficients that define the efficiency of converter $m \in \mathcal{M}$. Furthermore, the network presents different states that are being controlled, imposing constraints based on the linear system dynamics of the energy buffers

$$x_{m,k+1} = A_{m,k} x_{m,k} + B_{m,k} u_{m,k} \quad (1c)$$

in which $x_{m,k} \in \mathbb{R}^{n_m}$ and $u_{m,k} \in \mathbb{R}$ denote the predicted states and inputs, respectively, of subsystem $m \in \mathcal{M}$, and where the initial states $x_{m,0}$ are known. The admissible states and inputs are subject to constraints, i.e.,

$$x_{m,k} \in \mathcal{X}_m \text{ and } u_{m,k} \in \mathcal{U}_m \quad (1d)$$

Moreover, the interconnections of subsystems are described by $\mathcal{J} = \{1, \dots, J\}$ nodes and no direct interactions between them are considered, i.e., each subsystem can be connected only to a node, resulting in the power balances

$$g_j(y_{m,k}, u_{m,k}, w_{j,k}) \leq 0 \quad (1e)$$

with

$$g_j(y_{m,k}, u_{m,k}, w_{j,k}) = \sum_{m \in \mathcal{M}} c_{j,m} y_{m,k} + d_{j,m} u_{m,k} + w_{j,k} \quad (1f)$$

for all $j \in \mathcal{J}$ and $k \in \mathcal{K}$.

In (1e), $w_{j,k}$ are exogenous signals acting on each node, e.g., the power request from the driver or the auxiliaries. Generally for EMS, it is assumed that these exogenous signals are known in advance or can be perfectly predicted. However, this might not be always true, as they are generated by the environment or external factors, e.g., the driver. Therefore, we can consider that these unknown exogenous signals have a stochastic nature, turning the CVEM problem (1) into a Stochastic RHOC. Even though different methods can be used to solve this problem, we make use of the scenario approach (Campi and Garatti, 2018) to solve the resulting uncertain RHOC in a computationally advantageous way as presented in the remainder of this section (Detailed information on the CVEM framework can be found in Romijn et al. (2017)).

2.2 Stochastic RHOC

Before presenting the scenario approach, let us consider a stochastic extensions to problem (1) accounting for the unknown exogenous signals $w_{j,k}$ in nodes $j \in \mathcal{J}$. In particular, we can post the resulting CVEM problem as the following chance-constrained RHOC

$$\min_{\{u_{m,k}, y_{m,k}, x_{m,k}\}} \sum_{m \in \mathcal{M}} \sum_{k \in \mathcal{K}} a_{m,k} y_{m,k} + b_{m,k} u_{m,k} \quad (2a)$$

subject to (1b) - (1d), and

$$Pr\{g_j(y_{m,k}, u_{m,k}, w_{j,k}) \leq 0\} \geq 1 - \epsilon_j \quad (2b)$$

where the parameters ϵ_j are acceptable infeasibility levels and the functions g_j are defined as in (1e). Here, the need to guarantee that the chance-constraints (2b) will hold for any realization of $w_{j,k}$ becomes a major restriction, since the distributions of these exogenous signals might be unknown and, even if they are known, the solution could be more conservative and lead to an undesired performance.

2.3 Scenario-Based Traffic-Aware Energy Management

In order to deal with the characteristics of the chance-constrained formulation in the previous section, we make use of the scenario approach (Campi and Garatti, 2018) instead. This methodology for data-driven optimization aims to solve the resulting chance-constrained RHOCF by means of a deterministic approximation that considers only a finite number of realizations of the unknown exogenous signals $w_{j,k}$, where taking more samples into account increases the chances of satisfying (1e), thereby providing a tuning knob to balance robustness versus performance of the scenario solution. This allows to achieve a computationally tractable problem when multiple subsystems are considered, in comparison to classic stochastic EMS based on SDP (Johannesson et al., 2007). With this in mind, the power balances (2b) in problem (2) can be replaced by a deterministic set of randomly sampled constraints (scenarios), leading to what we refer to as scenario-based Traffic-aware Energy Management Strategy (ScTaEMS).

Now, following the scenario approach and the results in (Schildbach et al., 2013, 2014), we introduce some definitions and assumptions required for the scenario-based RHOCF:

- (1) The uncertainties $w_{j,k}$ of each node are contained in a single variable $w_k = [w_{1,k}, \dots, w_{J,k}]^\top$ which is a random variable with (maybe unknown) probability measure Pr and support set \mathcal{W} .
- (2) A sequence of variables $\{w_0^{[l]}, \dots, w_{K-1}^{[l]}\}$ is the l -th realization of the uncertainty w_k over the prediction horizon defining the scenario $w^{[l]}$.
- (3) Enough i.i.d. samples $w^{[l]}$ can be obtained at every time instant, giving a set of scenarios $\mathcal{I} = \{1, \dots, I\}$.
- (4) The scenario-based RHOCF problem has a feasible solution for almost any $w^{[l]}$.

With this definitions, the resulting scenario-based TaEMS problem at time $t \in \mathbb{N}$ is given by

$$\min_{\{u_{m,k}, y_{m,k}, x_{m,k}\}} \sum_{m \in \mathcal{M}} \sum_{k \in \mathcal{K}} a_{m,k} y_{m,k} + b_{m,k} u_{m,k} \quad (3a)$$

subject to

$$y_{m,k} = \frac{1}{2} \gamma_{2,m} u_{m,k}^2 + \gamma_{1,m} u_{m,k} + \gamma_{0,m} \quad (3b)$$

$$x_{m,k+1} = A_{m,k} x_{m,k} + B_{m,k} u_{m,k} \quad (3c)$$

$$x_{m,k} \in \mathcal{X}_m \quad \text{and} \quad u_{m,k} \in \mathcal{U}_m \quad (3d)$$

and

$$g_j(y_{m,k}, u_{m,k}, w_{j,k}^{[l]}) \leq 0, \quad (3e)$$

for all $l \in \mathcal{I}$ and $j \in \mathcal{J}$, and $k \in \mathcal{K}$, $m \in \mathcal{M}$.

From the previous formulation, we make use of the results in Schildbach et al. (2013) to address the selection of the number of scenarios required for a particular feasibility level. To this end, let us define the probability of constraint violation

$$V_{j,k}(y_{m,k}^*, u_{m,k}^*) = Pr\{g_j(y_{m,k}^*, u_{m,k}^*, w_{j,k}^{[l]}) > 0\} \quad (4)$$

where $u_{m,k}^*$, $y_{m,k}^*$ refer to the scenario solution. It has been shown in Campi and Garatti (2018) and Schildbach et al. (2013) that $V_{j,k}(y_{m,k}^*, u_{m,k}^*)$ is bounded by a Beta distribution $\mathbf{B}(\rho_j, I - \rho_j + 1)$, such that

$$Pr^I\{V_{j,k}(y_{m,k}^*, u_{m,k}^*) > \epsilon_j\} \leq \mathbf{B}(\rho_j, I - \rho_j + 1) \quad (5)$$

where ρ_j is the support rank of the constraint in node j and Pr^I is the I -th product of Pr for the sampled scenarios. Here, we make use of the results in Schildbach et al. (2013) instead of considering the number of decision variables as in the classic scenario approach presented in Campi and Garatti (2018). This is favorable as only a reduced number of the decision variables in problem (3) is affected by (3e) at every step on the prediction horizon k regardless of the number of sampled scenarios.

From this formulation, we aim to find the minimum number of samples required to satisfy the original chance constraint, as the more samples are drawn, the more conservative the solution becomes. Nevertheless, given that new samples are drawn at each time step, we consider a bound on the expected violation probability $\mathbb{E}^I[V_{j,k}(y_{m,k}^*, u_{m,k}^*)] \leq \epsilon_j$, which leads to a sample size of $\epsilon_j \leq \rho_j / (I + 1)$. This result follows from the integration of (5), which can be interpreted as the probability that the $I + 1$ sample becomes a support constraint, i.e., the solution obtained with the scenarios \mathcal{I} does not satisfy the power balances $g_j(\cdot) \leq 0$ (see Campi and Garatti (2018); Schildbach et al. (2013, 2014) for further details and proofs).

3. SCENARIO GENERATORS

In order to make predictions of the unknown traffic conditions, and thus the exogenous signals $w_{j,k}$, we present the three velocity prediction methods used in this work, e.g., predictions based on GPS/eHorizon data, predictions using a Gaussian Process Regression (GPR) model, and a mixed generator that combines both the GPS and the GPR model.

3.1 GPS / eHorizon Methods

First, we consider that the vehicle has access to traffic information through a Global Positioning System (GPS) or an electronic horizon (eHorizon), which are devices available in today's vehicles. Here, the average traffic speed is calculated based on the traffic flow through a particular section of the road as follows: $v_{avg,tw}^\eta = \frac{1}{P_\eta} \sum_{p=1}^{P_\eta} v_{tw}^p$, where η are the road sections and P_η is number of vehicles passing through a particular road section during a time window, e.g., an update frequency between 1 to 5 minutes, as is usually done in mapping and traffic management systems (HERE Global B.V, 2020; Herrera et al., 2010). Here, the generation of speed predictions assumes that the vehicle will follow the latest traffic speed recorded depending on the road section where it is located.

3.2 Gaussian Process Regression

Since the average traffic speed only provides a deterministic estimate of the traffic situation, a probabilistic model to forecast the future speed of the vehicle is proposed in this section. In particular, we propose to use a Gaussian Process Regression model (Rasmussen and Williams, 2006). The selection of this non-parametric model is motivated by the remarkable prediction capabilities achieved with machine learning methods in (Sun et al., 2015; Lefèvre et al., 2014; Liu et al., 2019) and, at the same time, its particular ability to provide a direct measure for the uncertainty of the predictions. For our application, the GPR model is employed as a predictor for a Nonlinear Auto-Regressive Model (NAR-GP), which results in regressing a function $\mathbf{z}_k = \mathbf{f}(\mathbf{q}_k) + \mathbf{e}_k$ with a feature vector $\mathbf{q}_k = \{v_{k-p}, \dots, v_k\}$ that predicts the future speed $\mathbf{z}_k = \{v_{k+1}\}$. Additionally, $\mathbf{e}_k \sim \mathcal{N}(0, \sigma_n^2)$ is a noise term acting on the output of the function and $\mathbf{f} \sim \mathcal{GP}(\mu, ker)$ is a GPR defined with a prior distribution with $\mu = 0$, a kernel function ker , e.g., squared exponential, Matérn, etc, and a set of hyper-parameters Θ . Furthermore, the definition of these hyper-parameters is done by minimizing the negative log-likelihood function on training data $\mathbf{D} = \{(q_n, z_n) \mid n = \{1, \dots, N\}\}$, see (Rasmussen and Williams, 2006) for further details.

Once the NAR-GP is fully defined, we obtain a model that allows us to generate random samples from the posterior distribution, such that

$$v_{k+1} \sim Pr(z_* | \mathbf{D}, q_*) = \mathcal{N}(\bar{f}_{post}, ker_{post} + \sigma_n^2; \Theta) \quad (6a)$$

in which

$$\bar{f}_{post} = ker^\top(q_*)(ker + \sigma_n^2 \mathbf{I})^{-1} \mathbf{z} \quad (6b)$$

$$ker_{post} = ker(q_*, q_*) - ker^\top(q_*)(ker + \sigma_n^2 \mathbf{I})^{-1} ker(q_*) \quad (6c)$$

with \mathbf{z} the output training data, \mathbf{I} the identity matrix and points q_* , z_* referring to a test input and output, respectively. For this method, we consider a *naive* approach to generate the predictions over the horizon \mathcal{K} , neglecting the propagation of uncertainty to simplify the process and avoid intractable predictions with large speed changes.

3.3 Mixed Generator Approach

Given that long prediction horizons lead to a better performance of the EMS (Romijn et al., 2017), a combination of the velocity prediction methods is considered in this work in order to exploit the benefits of each method, e.g., account for the uncertainty in a short-term and preserve the preview of the traffic situation given by the average traffic speed. This combination is motivated by the fact that most of the maneuvers in car following or traffic situations require a very short time (see Lefèvre et al. (2014) and references therein) and the possible mismatch between the traffic speed and the individual speed profiles. At the same time, it is known that machine learning methods tend to incur in large prediction errors when the prediction horizon length increases, as these methods are not able to account for long-term traffic dependencies (Liu et al., 2019). In fact, most of the methods present in the literature are restricted to predictions of 10 seconds in the future and, therefore, the integration of external information could lead to substantial fuel savings while generating more robust solutions against the actions of the driver.

Table 1. Powertain model coefficients

EGU		
$\gamma_{2,egu} = 2 \cdot 10^{-5}$	$\gamma_{1,egu} = 2.52$	$\gamma_{0,egu} = 19$
$\bar{u}_{egu} = 210$ [kW]	$\underline{u}_{egu} = 0$ [kW]	
HVB		
$\gamma_{2,hvb} = 1.671 \cdot 10^{-3}$	$\gamma_{1,hvb} = -1$	$\gamma_{0,hvb} = 0$
$\bar{u}_{hvb} = 92.4$ [kW]	$\underline{u}_{hvb} = -92.4$ [kW]	$x_{hvb,0} = 11988$ [kJ]
$\bar{x}_{hvb} = 22680$ [kJ]	$\underline{x}_{hvb} = 7560$ [kJ]	$x_{hvb,K} = 11988$ [kJ]

4. CASE STUDY

In this section, we define a simple case study considered to evaluate the potential of the proposed scenario formulation. The case study is based on TaEMS for a series hybrid vehicle. We will start by presenting the RHOCF formulation, followed by the selection of the sample size and the explanation of the power request determination.

4.1 Receding Horizon Optimal Control Problem

The case study in this paper is based on the series-hybrid electric vehicle (SHEV) presented in (Khalik et al., 2018). In particular, the powertrain topology of the vehicle is represented as the network of energy buffers depicted in Fig. 1b with $m = \{egu, hvb, em\}$. In this figure, EGU stands for Engine Generator Unit, with y_{egu} being the fuel consumption and u_{egu} the power supplied by the EGU to the power network. Furthermore, u_{hvb} and y_{hvb} define the electric power coming from the High-Voltage Battery (HVB) and x_{hvb} represents the stored energy in the battery. Besides this subsystems, the Electric Motor (EM) provides y_{em} , which represents the (unknown) power request defined by the driver. Note that y_{em} propels the vehicle when being positive and brakes the vehicle when being a negative value.

The node interconnecting the elements in the network defines a power balance as in (1e), where the parameters $c_{hvb} = 1$, $d_{egu} = -1$ and $c_{em} = 1$ are specified according to the flow direction of the power for each subsystem and all the others are set to zero. On top of this, an external braking signal y_{br} is introduced to account for the mechanical braking that dissipates the excess of energy in the powertrain and $x_{hvb,0} = x_{hvb,K}$ is included in (3d).

According to the problem formulation in Section 2.1, the task of reducing the fuel consumed by the SHEV is described by the cost function (1a) with $a_{egu,k} = \tau_k$ and all the remaining parameters $a_{m,k} = b_{m,k} = 0$, as they do not contribute to the objective of the problem and where τ_k is the sampling interval along the prediction horizon \mathcal{K} . In this case, $y_{em,k}$ is considered to be an uncertain consequence of the driver actions and only the power request $y_{em,0}$ is known at the current time step t , which is a realistic assumption given the on-board sensors in today's vehicles. Furthermore, Table 1 presents the parameters defining the powertrain in this case study.

By substituting (3b) for the EGU in (3a) and (3b) for the HVB in (3e), removing the state variables through a prediction model as is generally done in linear MPC and considering the case study's parameters, the problem can be reformulated as a Quadratically Constrained Quadratic Program (QCQP) which can be efficiently solved with specialized solvers, e.g., CPLEX CPL (2019), resulting in

$$\min_{\{u_{m,k}\}} \sum_{k \in \mathcal{K}} \tau_k \left(\frac{1}{2} \gamma_{2,egu} u_{egu,k}^2 + \gamma_{1,egu} u_{egu,k} + \gamma_{0,egu} \right) \quad (7a)$$

subject to

$$\underbrace{\frac{1}{2} \gamma_{2,hvb} u_{hvb,k}^2 + \gamma_{1,hvb} u_{hvb,k} - u_{egu,k} + \gamma_{0,hvb}}_{g_{qcqp}} \leq -y_{em,k}^{[l]} \quad (7b)$$

for all $l \in \mathcal{I}$ and

$$\Phi x_{hvb,0} - \tau_k \circ \Gamma \mathbf{u}_{hvb} \in \mathcal{X}_{hvb} \quad (7c)$$

$$u_{m,k} \in \mathcal{U}_m \quad (7d)$$

with $k \in \mathcal{K}$, $m \in \{egu, hvb\}$ and (7c) are the battery constraints in matrix form. Note that this problem is convex since $\gamma_{2,m} > 0$, leading to a direct definition of the sample size for the scenario-based RHOC. P

4.2 Sample Size for Scenario-based RHOC. P

Since the power balance (7b) is present for every prediction of time $k + t$, given information at time t , the problem has K scenario constraints and affect only the particular inputs at that stage in horizon \mathcal{K} . Therefore, it is straightforward to define the support rank of the scenario constraint and specify the required sample size. In this case, the support rank of (7b) is calculated as in Schildbach et al. (2013) and given by $\rho = d - \mathcal{L} = 2$, leading to an expected violation probability $\mathbb{E}^I[V_{j,k}(u_{m,k}^*)] \leq \frac{2}{I+1}$, where $V_{j,k}(u_{m,k}^*) = Pr\{g_{qcqp} + (\gamma_{0,hvb} + y_{em,k}^{[l]}) > 0\}$. In this case study, we have defined a sample size of $I = 119$ implying a theoretical bound of $\epsilon \leq 2/120 \approx 1.66\%$. This percentage can be interpreted as the times when the vehicle will not provide enough power to follow the commands of the driver.

4.3 Power Request Definition

Given that the scenario generators forecast possible velocity profiles $\{v_1, \dots, v_{K+1}\}$, the power request is considered as the mechanical power $y_{em,k} = v_k u_{em,k}$, where a power limit $\bar{y}_{em} = \bar{u}_{egu} + \bar{y}_{hvb}$ is defined and the traction force, $u_{em,k}$, required to follow each profile is calculated using an inverted vehicle dynamics model, given by:

$$y_{em,k} = \frac{v_k}{\sigma_u} \left(\frac{v_{k+1} - v_k}{\tau_k} + \sigma_v v_k^2 + \sigma_r + g \sin(\theta(s_k)) \right) \quad (8)$$

where $\sigma_r = g c_r$, $\sigma_u = \frac{1}{m}$, $\sigma_v = \frac{1}{2m} c_d \rho_a A_f$ and θ define the rolling resistance, inverse of the mass, aerodynamic drag and the road slope, respectively. The definition and values of these coefficients for the vehicle in this case study can be found in Table 2 and a flat road is considered, i.e., $\theta = 0$.

5. SIMULATION RESULTS

In order to analyse the performance of the scenario generators and the TaEMS for the power split problem, we first describe the particular characteristics considered in the simulations and, subsequently, we present results obtained with each method. Here, the solutions of the TaEMSs are compared to the optimal performance given by an offline benchmark and an online solution with perfect prediction of the future driving cycle. Additionally, we assess the benefits of hybridization under uncertain predictions by

Table 2. Vehicle coefficients

Parameter	symbol	Value
Frontal drag area	A_f	7.5400 [m^2]
Drag coefficient	c_d	0.7
Rolling resistance	c_r	0.007
Air density	ρ_a	1.1840
Mass	m	15950 [kg]
Gravitational acceleration	g	9.81 [m/s^2]

including the fuel consumption that would be generated if the power request was only covered by the EGU.

For this case study, we used the traffic data set from the *Mobile Century* field experiment (Herrera et al., 2010), which was a project carried out over a 16 km section of the Interstate 880 highway in California to evaluate the use of GPS-enabled smartphones for accurate traffic information systems. The data was recorded from 10 a.m. to 6 p.m. and includes a traffic congestion event around 10:30 a.m. from where the driving cycles to evaluate the proposed TaEMS are taken (the reader is referred to Herrera et al. (2010) for further information and descriptions of the data used).

For implementation, we use a moving average filter with a Gaussian window to smooth intractable speed changes present in the predictions from the traffic speed or large noise realizations in the NAR-GP samples.

5.1 GPS / eHorizon Method

In order to replicate the information supplied by a GPS, we have divided the road in 100 segments and have considered a time window $tw = 300$ seconds according to the update frequency in (Herrera et al., 2010). We consider that the vehicle has access to the average speed relative to the current time relative to the driving cycle, e.g., at 10:43 a.m. the information obtained at 10:40 a.m. is known and an update is available at 10:45 a.m.

5.2 Gaussian Process Regression

For this probabilistic velocity prediction method, the training data \mathbf{D} was composed by real driving cycles taken from the *Mobile Century* data set starting before 10:30 a.m., and the HWFET, LA92 short and EPA standard driving cycles in order to provide more dynamic data to the model. Furthermore, the kernel function used in this work is the *Matérn* $_{\frac{5}{2}}$ function, see, e.g., (Rasmussen and Williams, 2006). This selection was motivated by the fact that the real driving cycles present long braking patterns, which were not properly captured when using a squared exponential function due to its smoothness characteristics. Additionally, the total number of lags in the NAR-GP was set to 5, since it was observed that longer dependencies did not provide a substantial improvement of the predictions.

As an example, the mean predictions generated with the NAR-GP for test cycle 1 are shown in Fig. 2, where the top plot presents the prediction accuracy with different prediction horizons and the trajectories for 10 seconds of prediction are shown in the bottom plot. As it can be seen, when the predictions are made for short periods of time, e.g., 10 seconds, 95% of the errors are smaller than 1 m/s, which is acceptable for the development of energy management strategies. Nevertheless, these errors

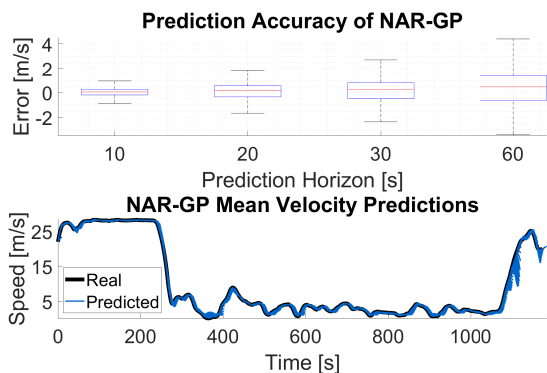


Fig. 2. NAR-GP predictions for test cycle 1. Top: Error of the predicted mean vs. prediction horizon length. Bottom: Predicted mean speed with $K = 10$ seconds.

present an increasing trend when generating a velocity forecast for longer horizon lengths, as only short term correlations are captured from the training data and translated to the predictions while no information of the upcoming traffic is provided to the NAR-GP. Besides this, the NAR-GP occasionally generates wrong braking predictions, e.g., predictions around second 1100, but such errors are mitigated by the presence of multiple random samples that result in a more cautious use of the battery.

5.3 Prediction Horizon Length

In order to establish an appropriate length of the prediction horizon, the fuel consumption obtained with the GPS and the NAR-GP predictions were evaluated. Table 3 presents the fuel consumption with a perfect prediction, the scenario solution with the NAR-GP and the average traffic speed (GPS), where the offline benchmark and the EGU-only case (i.e., not using the battery) give the range of possible savings. It can be seen that a longer prediction horizon results in a lower consumption since it allows a larger deviation from the final state constraint imposed in the problem. For test cycles 1 and 2, the GPS captures the braking pattern accurately, leading to an appropriate use of the battery compared to the NAR-GP, where the battery is mainly used after the charging event due to prediction errors, see Fig. 3. Regarding the third test, the GPS

Table 3. Impact of prediction horizon on fuel consumption for the individual methods

Method	Horizon Length [seconds]	Fuel Consumption per Test Cycle [l]/100[km]		
		1	2	3
Offline	-	21.104	24.666	20.310
EGU-only	-	23.390	26.222	21.978
Perfect Prediction	20	22.101	25.689	20.872
	30	21.759	25.327	20.625
	60	21.166	24.748	20.362
	120	21.121	24.684	20.322
NAR-GP	20	22.951	25.731	21.282
	30	22.795	25.482	21.074
	60	22.312	25.353	20.553
	120	22.006	25.160	20.506
GPS	20	22.718	25.836	20.973
	30	22.444	25.459	20.889
	60	22.084	25.003	20.618
	120	21.702	24.947	20.766

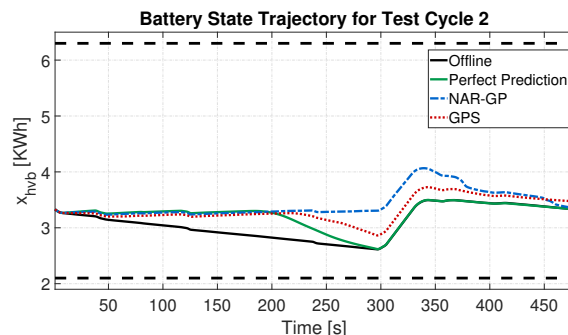


Fig. 3. Trajectory of the energy stored in the battery for test cycle 2 (battery limits are shown as dashed lines)

incurs in a higher consumption with longer predictions, while the NAR-GP leads to better fuel economy. This is due to a softer deceleration that deviates from the traffic flow and, as seen in the perfect prediction case, reduces the advantage of a long horizon compared to the other tests.

5.4 Mixed Scenario Generator

As shown before, the NAR-GP is capable of producing accurate predictions when a short horizon is specified but fails to anticipate longer braking events, causing a higher fuel consumption. For this reason, and as a reference point with the literature, a horizon length of 10 seconds was selected to generate random speed profiles. After these predictions are made, the average traffic speed is used to complete the remaining part of the prediction horizon assuming that the driver follows the GPS after 10 seconds in order to keep the preview of the future traffic conditions and provide more freedom for the usage of the battery.

Finally, since longer horizons have a large impact in the computation time due to the increment of constraints and decision variables in the RHOCP, we incorporate the variable step-size approach proposed in (Romijn et al., 2017) since, as indicated by the authors, coarser predictions of the future have minor impacts in the fuel savings while noticeably reducing the computation complexity of the problem. We consider $(\tau_1, \dots, \tau_K) = (1, 1, 2, 4, 6, 8, 10, 12, 16, 20, 40)$ as the step-size sequence used to generate long-term predictions, where the specific sequence follows the suggestion in (Romijn et al., 2017), such that the total length of the predictions is 120 seconds.

The resulting fuel savings obtained with the mixed scenario generator are reported in Table 4, where we present the fuel consumed with ‘full mixed’ scenario generator (i.e.,

Table 4. Fuel consumption of TaEMS with mixed scenarios and GPS information

Test Cycle	Method	Fuel [l]/100[km]	Relative Fuel Consumption Increase
1	Full Mixed	21.674	2.70 %
	Variable Mixed	21.852	3.54 %
	Variable GPS	22.220	5.29 %
2	Full Mixed	24.851	0.75 %
	Variable Mixed	25.109	1.79 %
	Variable GPS	25.423	3.06 %
3	Full Mixed	20.804	2.44 %
	Variable Mixed	21.247	4.62 %
	Variable GPS	21.136	4.07 %

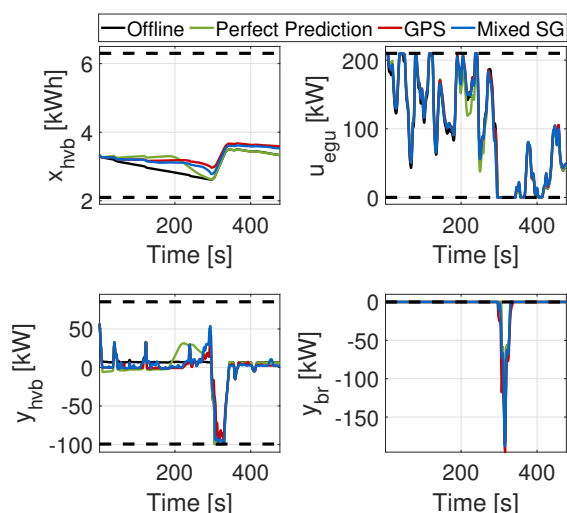


Fig. 4. State trajectory and node signals from the TaEMSs using sequence τ_k in test cycle 2 (dashed lines: limits).

with constant step sizes $\tau_k = 1$), the ‘variable mixed’ scenario generator (i.e., with variable step sizes, as explained above) and applying the same variable step size sequence only to the average traffic speed, i.e., ‘variable GPS’. Here, the last column presents the increment of fuel consumption relative to the optimal savings of the offline benchmark. Moreover, the state trajectory and the signals acting on the powertrain node in test cycle 2 are shown in Fig. 4.

From Table 4, it can be seen that the proposed TaEMS provides a slight improvement when the full predictions of the mixed scenario generator are considered in comparison to the GPS-based predictions. Nevertheless, the main advantage is observed when the decision variables are reduced by means of the variable sequence τ_k . In this case, we see that the fuel savings decreased as shown in (Romijn et al., 2017) but the incorporation of multiple predictions leads to a better fuel economy, consuming only 0.75% more than the optimal solution in test cycle 2 when full predictions are used and 1.79% with the sampling sequence τ_k . On the other hand, the negative effect of faulty predictions is also visible, as the consumption increases due to the mismatch of the long-term predictions in test cycle 3.

6. CONCLUSIONS

In this paper, a traffic-aware energy management strategy that accounts for uncertain driving conditions has been developed. This strategy is based on the solution to a scenario-based optimal control problem used in a receding horizon fashion. The scenario-based approach reduces the probability of running out of energy during a driving mission. Different alternatives to include traffic information for the generation of scenarios have been explored, achieving a deviation of 0.75% from the optimal consumption with a suitable mix of the available information and 1.79% using variable step-size predictions. Nevertheless, the need of accurate traffic data becomes an essential factor for this TaEMS, however, such quality of information was provided by the traffic behavior in the highway situation considered.

REFERENCES

IBM ILOG CPLEX V12.9 Users Manual for CPLEX, 2019.

- M. C. Campi and S. Garatti. *Introduction to the Scenario Approach, Volume 26 of MOS-SIAM Series on Optimization*. SIAM, 2018.
- S. Di Cairano, D. Bernardini, A. Bemporad, and I. V. Kolmanovsky. Stochastic MPC With Learning for Driver-Predictive Vehicle Control and its Application to HEV Energy Managements. *IEEE Trans on Control Syst Techn*, 2014.
- HERE Global B.V. HERE Real-Time Traffic. <https://www.here.com/products/traffic-solutions/real-time-traffic-information>, 2020. Online; accessed 28-04-2020.
- J.C. Herrera, D. Work, R. Herring, X. Ban, Q. Jacobson, and A.M. Bayen. Evaluation of traffic data obtained via gps-enabled mobile phones: The mobile century field experiment. *Transportation Research Part C: Emerging Technologies*, 2010.
- IEA. Global EV Outlook 2018. Technical report, International Energy Agency, 2018.
- L. Johansson, M. Asbogard, and B. Egardt. Assessing the Potential of Predictive Control for Hybrid Vehicle Powertrains Using Stochastic Dynamic Programming. *IEEE Trans on Intell Transportation Syst*, 2007.
- J. Kessels, J. Martens, P. van den Bosch, and W. Hendrix. Smart vehicle powernet enabling complete vehicle energy management. In *Proc of the Vehicle Power and Propulsion Conf*, 2012.
- Z. Khalik, G.P. Padilla, T.C.J. Romijn, and M.C.F. Donkers. Vehicle Energy Management with Ecodriving: A Sequential Quadratic Programming Approach with Dual Decomposition. In *Proc American Control Conf*, 2018.
- S. Lefèvre, C. Sun, R. Bajcsy, and C. Laugier. Comparison of parametric and non-parametric approaches for vehicle speed prediction. In *Proc American Control Conf*, 2014.
- K. Liu, Z. Asher, X. Gong, M. Huang, and I. Kolmanovsky. Vehicle Velocity Prediction and Energy Management Strategy Part 1: Deterministic and Stochastic Vehicle Velocity Prediction Using Machine Learning. *SAE Technical Paper*, 2019.
- G.P. Padilla, G. Belgioioso, and M.C.F. Donkers. Global solutions to the complete vehicle energy management problem via forward-backward operator splitting. In *Proc Conf on Decision and Control*, 2019.
- C. E. Rasmussen and C. K. I. Williams. *Gaussian Processes for Machine Learning*. The MIT Press, 2006.
- T.C.J. Romijn, M.C.F. Donkers, J.T.B.A. Kessels, and S. Weiland. Real-time distributed economic model predictive control for complete vehicle energy management. *Energies*, 2017.
- G. Schildbach, L. Fagiano, and M. Morari. Randomized Solutions to Convex Programs with Multiple Chance Constraints. *SIAM Journal on Optimization*, 2013.
- G. Schildbach, L. Fagiano, C. Frei, and M. Morari. The scenario approach for stochastic model predictive control with bounds on closed-loop constraint violations. *Automatica*, 2014.
- A. Sciarretta and L. Guzzella. Control of hybrid electric vehicles. *IEEE Control Systems Magazine*, 27(2):60–70, 2007.
- C. Sun, X. Hu, S.J. Moura, and F. Sun. Velocity predictors for predictive energy management in hybrid electric vehicles. *IEEE Trans on Control Syst Techn*, 2015.